IX. MANGANESE NODULES AND BENTHONIC ACTIVITIES BY DEEP SEA PHOTOGRAPHY

Yasumasa Kinoshita

Introduction

Several hundreds of deep sea bottom pictures were obtained at the Central Pacific stations, Sts. 408A-1 (C7) and 414A-3 (C6). The still camera used was an Edgerton 35 mm deep sea camera (Model 372) combined with an deep sea electronic flash (Model 382), both manufactured by Benthos Inc. (Fig. IX-1). A sonar pinger was used for monitoring the underwater camera position in the same way as described by YAMAKADO *et al.* (1975).

During the operation of the camera system, the pinger records on PDR were continuously monitored to keep the camera 1–2 m above sea bottom. Many clear pictures were obtained at the two stations, and provide useful data to analyze the distribution and occurrence of manganese nodules associated with evidence of intensive benthonic activity. Also, it is particularly noticeable that both the features of nodules and benthonic activities are fairly different each other at the two stations.

Photography at St. 408A-1 was done at 10 sec. intervals for 2 hours and 16 minutes, resulting in 147 frames of pictures which intermittently cover the extent of 630 m of sea bottom. The calculation by magnetic compass simultaneously figured shows that the ship was drifting towards north-northeast with a speed of 0.15 knot (Fig. IX-2). This is in harmony with the result of recalculation of NNSS data by ISHIHARA (in this report). On the pictures the distribution of a great amount of manganese nodules with very high coverage can be seen.

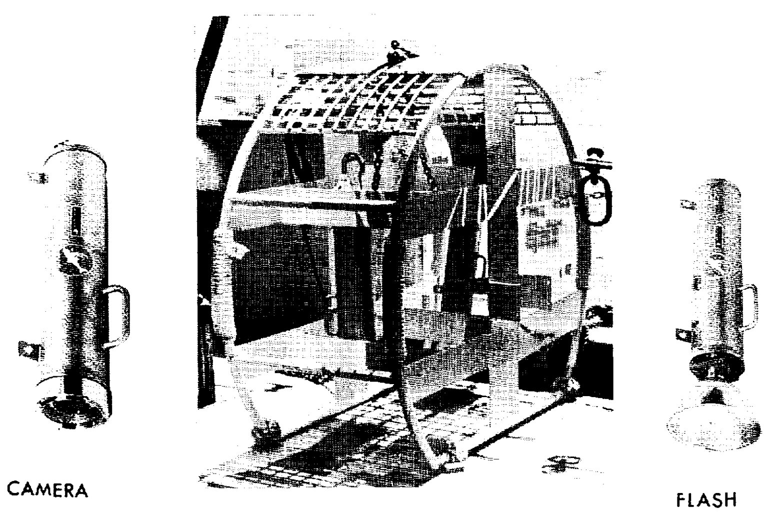

Fig. IX-1 Deep sea camera and electronic flash used in GH76-1 cruise.

Table IX-1 Location, depth, and photographing condition.

Station no.	St. 408A–1	St. 414A–3
Location	09°–59.3N 174°–00.5W	04°–59.1N 172°–59.0W
Depth	5,820 m	5,410 m
Photographing condition		
Distance	2 m	2 m
F. stop	5.6	5.6
Film	KODAK PLUS-Pan Film black-and-white 100 ft ASA 125	KODAK PLUS Pan Film black-and-white 100 ft ASA 125
Photographing interval	10 sec.	3 sec.
Photographing time	2 h 16 min.	23 min.

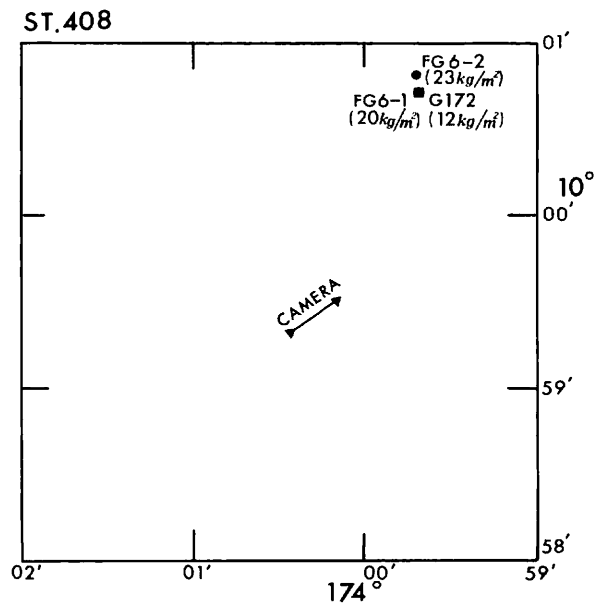

Fig. IX-2 Location of photography at St. 408A-1.

The pictures at St. 414A-3 were obtained by photographing at 3 sec. intervals for 23 minutes with the ship drifting to the northwest, and 300 frames of pictures were taken over a sea bottom extent of 110 m. The drifting direction calculated in the same way as above shows a great discrepancy with the recalculated general direction by NNSS after ISHIHARA (see Fig. II-12 and IX-3). This might be caused by too short a time interval of photographing for the total time range and distance of NNSS positioning. In contrast to the preceding station, the less dense, scattered distribution of nodules are observed throughout the pictures.

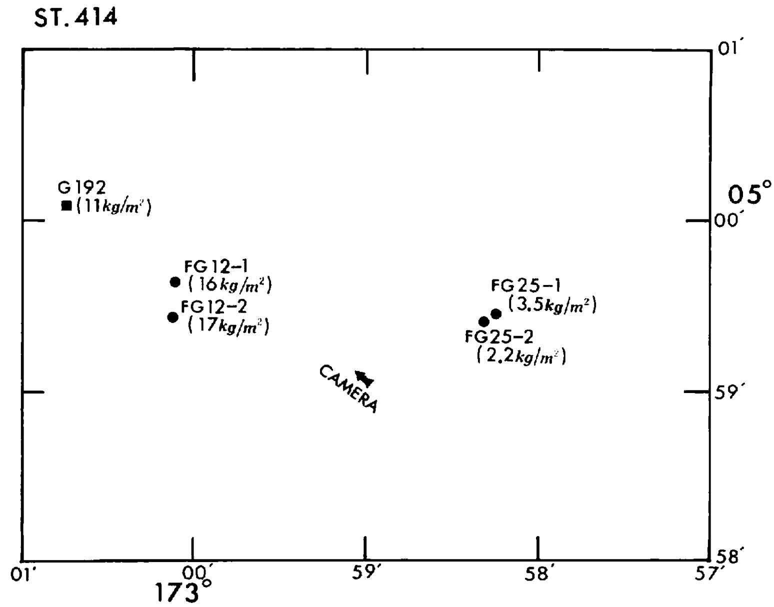

Fig. IX-3 Location of photography at St. 414A-3.

The manganese nodules on the pictures obtained were observed by means of a photo pattern analyzer particularly concerning coverage and abundance. Also their arrangement, size, and elongation were measured.

Manganese nodules

The pictures at St. 408A-1 show that abundant nodules are nearly uniformly distributed with about 70% coverage over the sea floor of approximately 630 m in distance (Figs. IX-4, 5). Concerning the size frequency, as shown in Table IX-2, 95% of nodules consist of those larger than 2.5 cm, and 56.9% are represented by those of the size class of 2.5–5.0 cm. The results of coverage and size frequency analyses seem to be in harmony with the sampling data of FG6-2 and FG6-1 that show 20–23 kg/m² abundance (Fig. IX-2) at about 2.8 km northeast away from the photographed bottom. Also the morphological observation of the photographed nodules shows their attribution to IDPs and DPs (Moritani *et al.*, in this report) in larger part as well as the sampled nodules.

The result of orientation analysis on 1049 pieces of nodule on the pictures indicates that the mean value of the elongation axis of the nodules is −32.6° with a standard deviation of 50.5° (Fig. IX-6). In this measurement, a standard deviation of less than 50.0° would be required for a preferred orientation with a probability of 5%. Therefore it is concluded that there is no recognizable preferred orientation of nodule arrangement at St. 408A-1. If a hydraulic action influenced the formation of nodules, any preferred orientation would be present. The result provides evidence of the non-existence of any significant bottom current related with the arrangement of nodules. Moreover, as the nodule morphology is largely controlled by the shape of the nucleus, an original

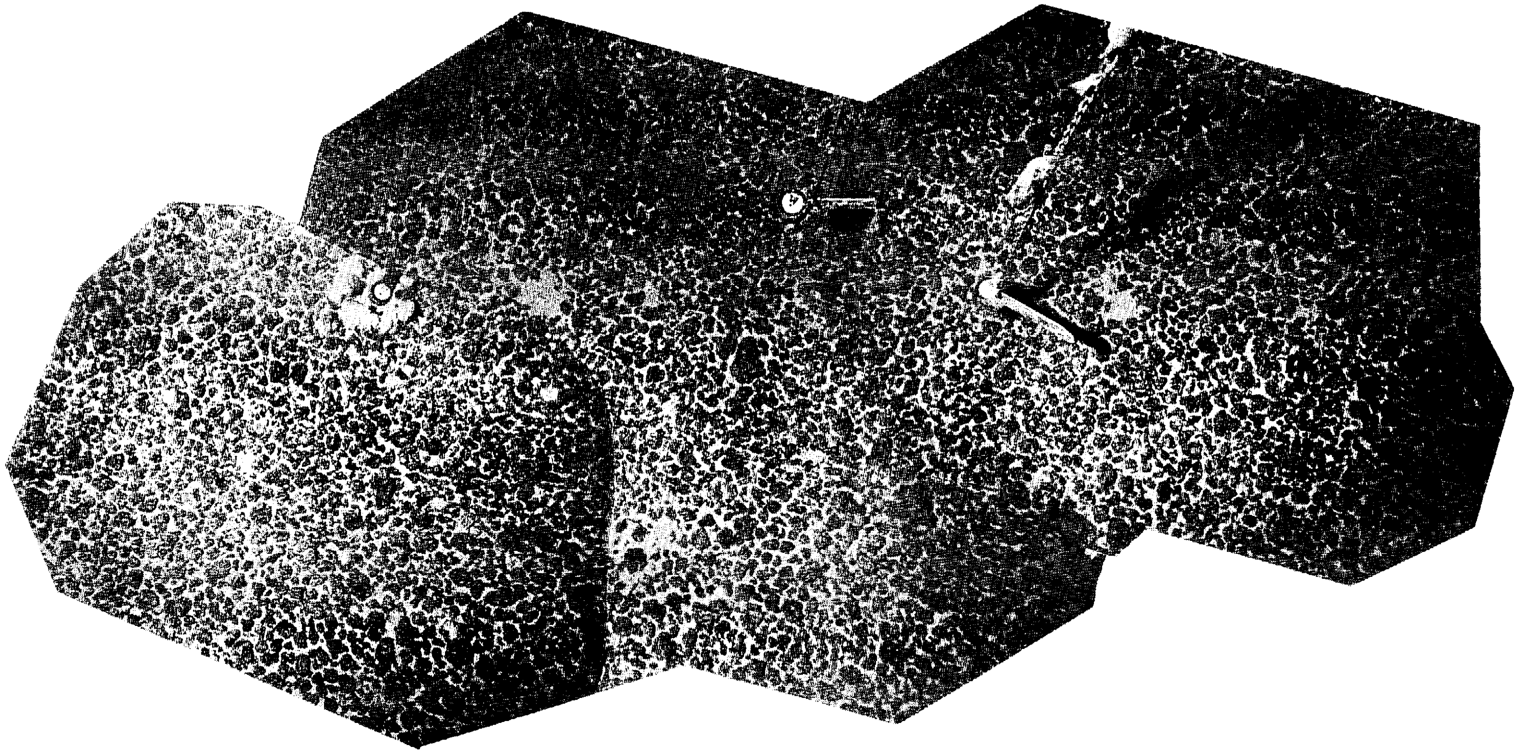

1 M ST. 408

Fig. IX-4 Continuous pictures of sea bottom covered with abundant nodules at St. 408A-1.

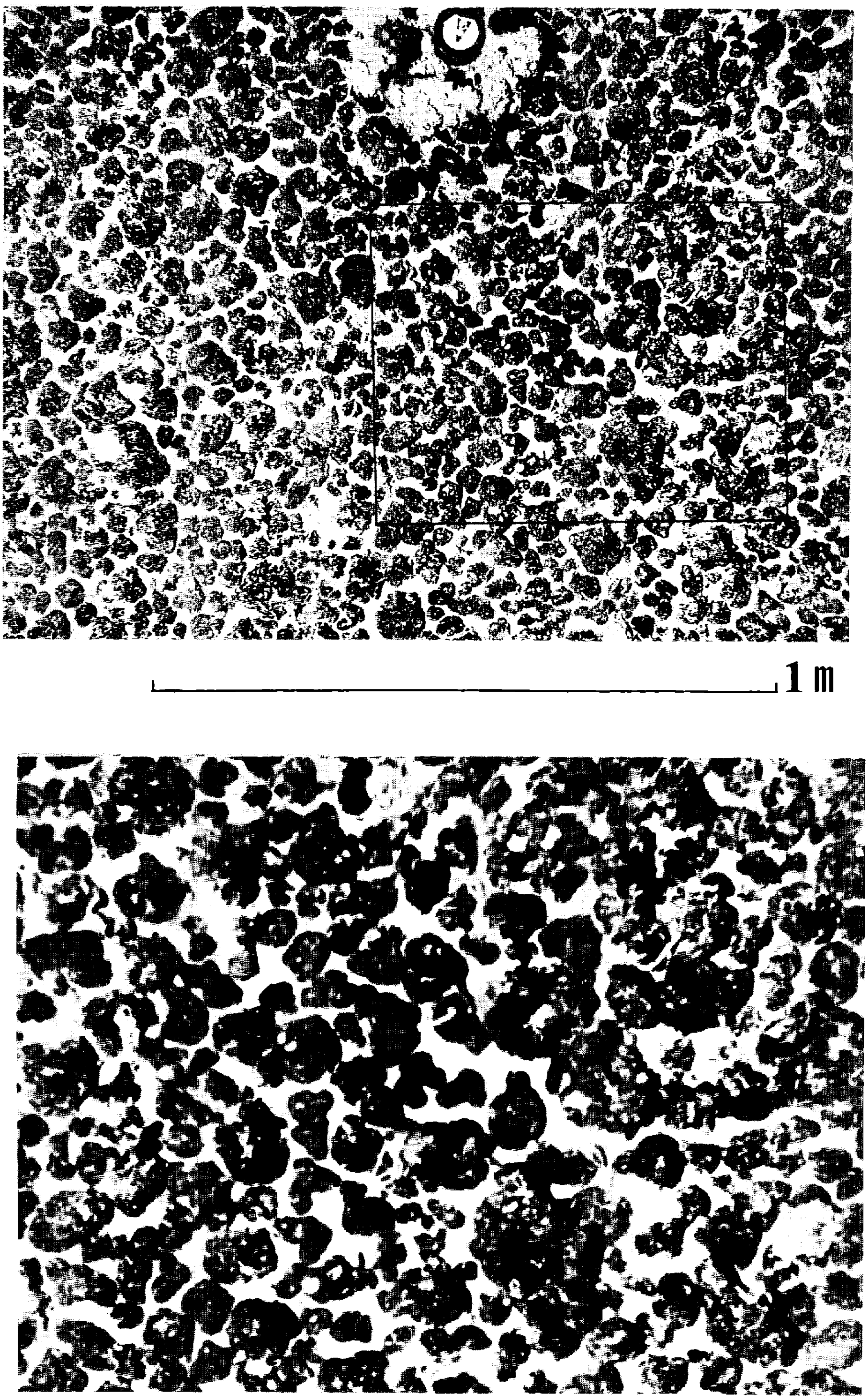

Fig. IX-5 A part of pictures at St. 408A-1.
The lower figure shows the enlarged one of the quadrangle of solid line in the upper figure.

Table IX-2 The number of the each size class for per unit area.

St. 408-A

	Frame no. 30		Frame no. 110	
10 cm<	4	0.9%	4	0.8%
10 ~ 7.7 cm	22	4.8%	25	5.2%
7.5 ~ 5.0 cm	147	32.2%	155	32.4%
5.0 ~ 2.5 cm	260	56.9%	272	56.9%
2.5 cm>	24	5.3%	22	4.6%
Total	457		478	

St. 414A-3

	Frame no. 17		Frame no. 20	
10 cm<	0	0%	0	0%
10 ~ 7.5 cm	9	5.8%	3	2.1%
7.5 ~ 5.0 cm	24	15.4%	22	15.4%
5.0 ~ 2.5 cm	85	54.5%	93	65.0%
2.5 cm>	38	24.4%	25	17.5%
Total	156		143	

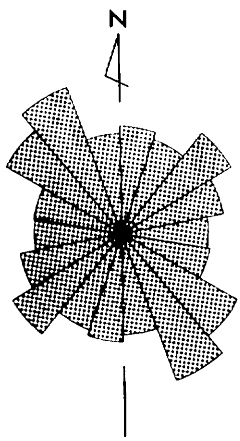

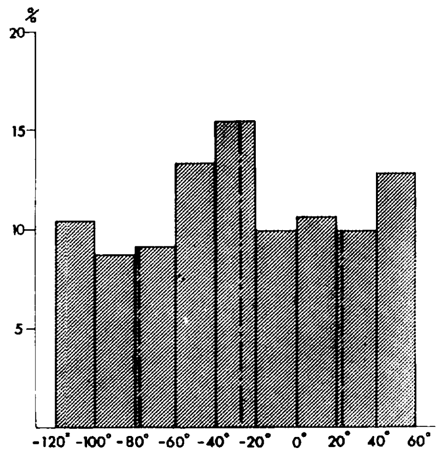

Fig. IX-6 Orientation of elongation axis of manganese nodules at St. 408A-1.

arrangement of such nucleus' on the sea bottom has also not been affected by any significant bottom current.

The manganese nodules are semi-buried in the surficial sediments. The pictures show that the sediments include much evidence of organic activity such as coprolites, trails, etc. Coprolites are also found also on nodules, and they are nearly perfectly preserved in some cases, but are markedly collapsed in other cases.

The pictures at St. 414A-3 (Figs. IX-7, 8) show that the nodules are less densely concentrated over the extent of the 110 m transect. with a coverage of 37% at the beginning of the series of photographs, decreasing to 25% at the last. As shown in Table

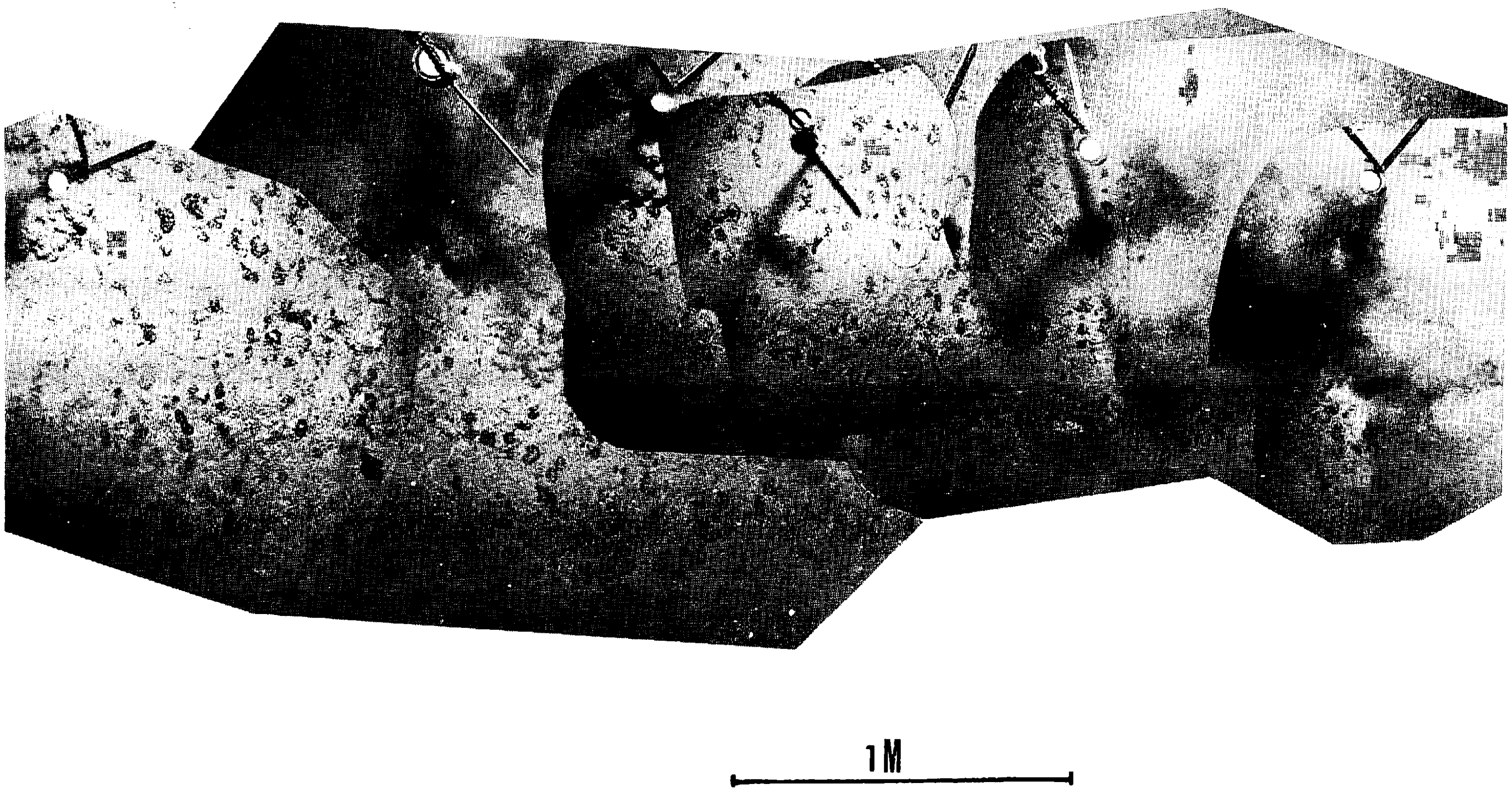

Fig. IX-7 Continuous pictures of sea bottom with scattered nodules at St. 414A-3.

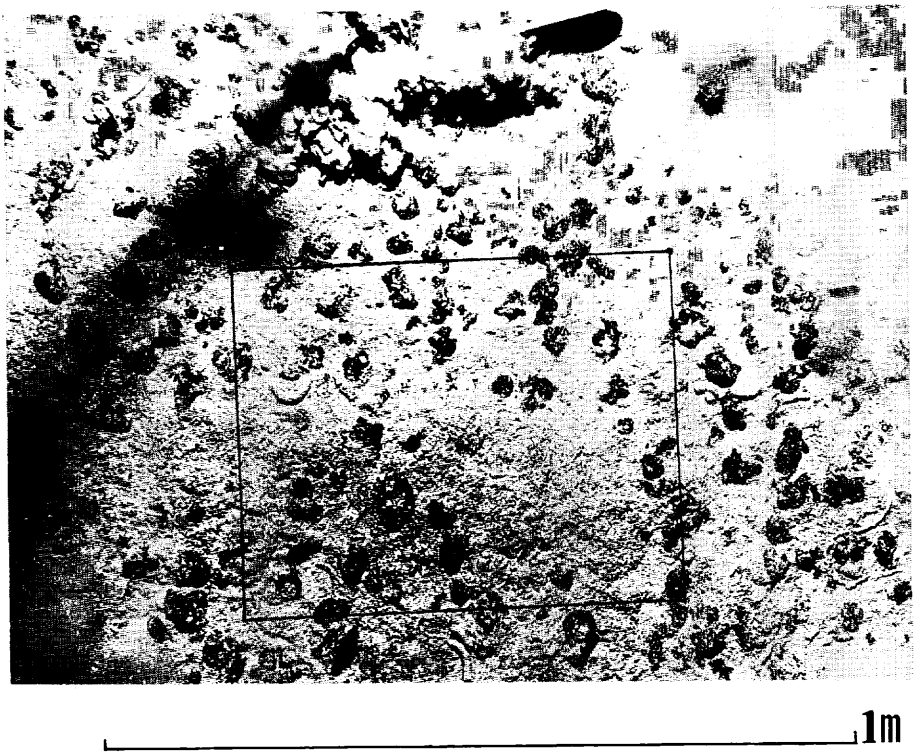

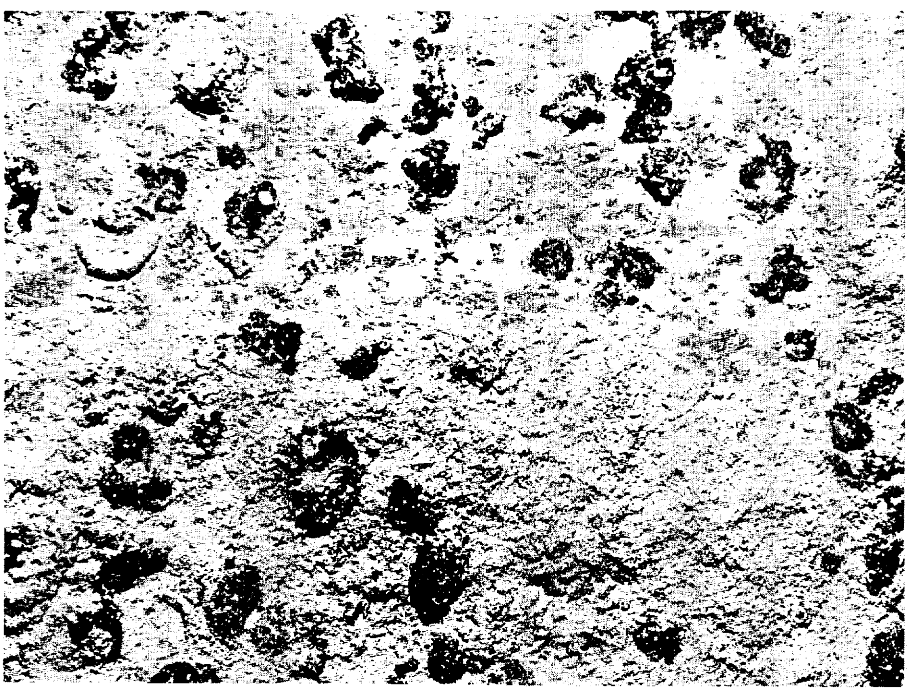

Fig. IX-8 A part of pictures at St. 414A-3.
The lower figure shows the enlarged one of the quadrangle of solid line in the upper figure.

IX-2, the nodules with 2.5–5.0 cm occupy 55–65% of the total and those larger than 2.5% attain 75–83%, thus being largely smaller than those at St. 408A-1. The nodules seem to belong to the morphological type, DPs (after MORITANI *et al.*, in this report), similar to those sampled at St. 414 (FG12-1, 2) and St. 414A (G193) 2–4 km to the northwest, while the measured coverage suggests that their abundance seems to decrease towards the southeast within the extent of distribution of nearly single type—s-group (MORITANI *et al.*, in this report)—. At any rate, it is unlikely that a series of nodule distribution continues to St. 414A-2 (FG25-1, 2) about 1.8 km away to the NE where a very low concentration of nodules of the Sr type is found (see Fig. IX-3). There might be expected a discontinuous boundary of nodule type and abundance between the photographed bottom and St. 414A-2. No definite evidence of bottom current affecting the nodule genesis is recognized on the pictures at St. 408A-3 as well as at St. 408A-1. Evidence of benthonic activity is fairly abundant at the present station in comparison to that at St. 408A-1.

Benthonic activity

Evidence of benthonic activity is abundant on the pictures obtained, and can be summarized briefly as follows. Benthonic activity is indicated by organic bodies, trails, nests, and coprolites at both the stations. Coprolites with various morphology are generally dominate.

Organisms

Organic bodies are rather poorly represented by some benthonic forms with sizes of several centimeters to around 10 cm. They are largely classified into at least seven kinds (Fig. IX-9). They include some species of arthropods (Fig. IX-9-1, 2), ophiuroids (Figs. IX-9-4, 11), ? sea cucumbers (Figs. IX-9-3, 6, 9) and inderterminable organisms (Figs. IX-9-5, 7, 8, 10). Some similar forms are also illustrated in the report by HORN *et al.* (1973, p. 56) as the life on siliceous deposits, thus showing the extensive activities of some particular benthonic organisms on the deep sea bottom associated with abundant or less manganese nodules.

Trails, nests, or burrows

Lebensspuren such as trails, nests, or burrows, except coprolites, are generally classified into five ecological types of repichnia, pascichnia, fodinichnia, domichnia, and cubichnia (SEILACHER, 1953; HANTSCHEL, 1962), each of which shows characteristic impressions.

Among the five types, repichnia, cubichnia, and domichnia are found in the pictures from St. 414A-3 and they are illustrated by the symbols of a, b, and c, respectively, in Fig. IX-10. Unfortunately their original animals are uncertain as yet.

They disappear from the pictures at St. 408A-1, where many coprolites are found. They may be burried by the dense covering of manganese nodules.

Coprolites

Evidence of benthonic activity exclusively by coprolites is shown in the pictures of St. 408A-1. At this station, the coprolites are tentatively classified into nine morphological types (A-H in Figs., IX-11 and 12). Most of the coprolites are found on the surface of manganese nodule, showing that the benthonic activity which produced the coprolites occurred after nodule formation.

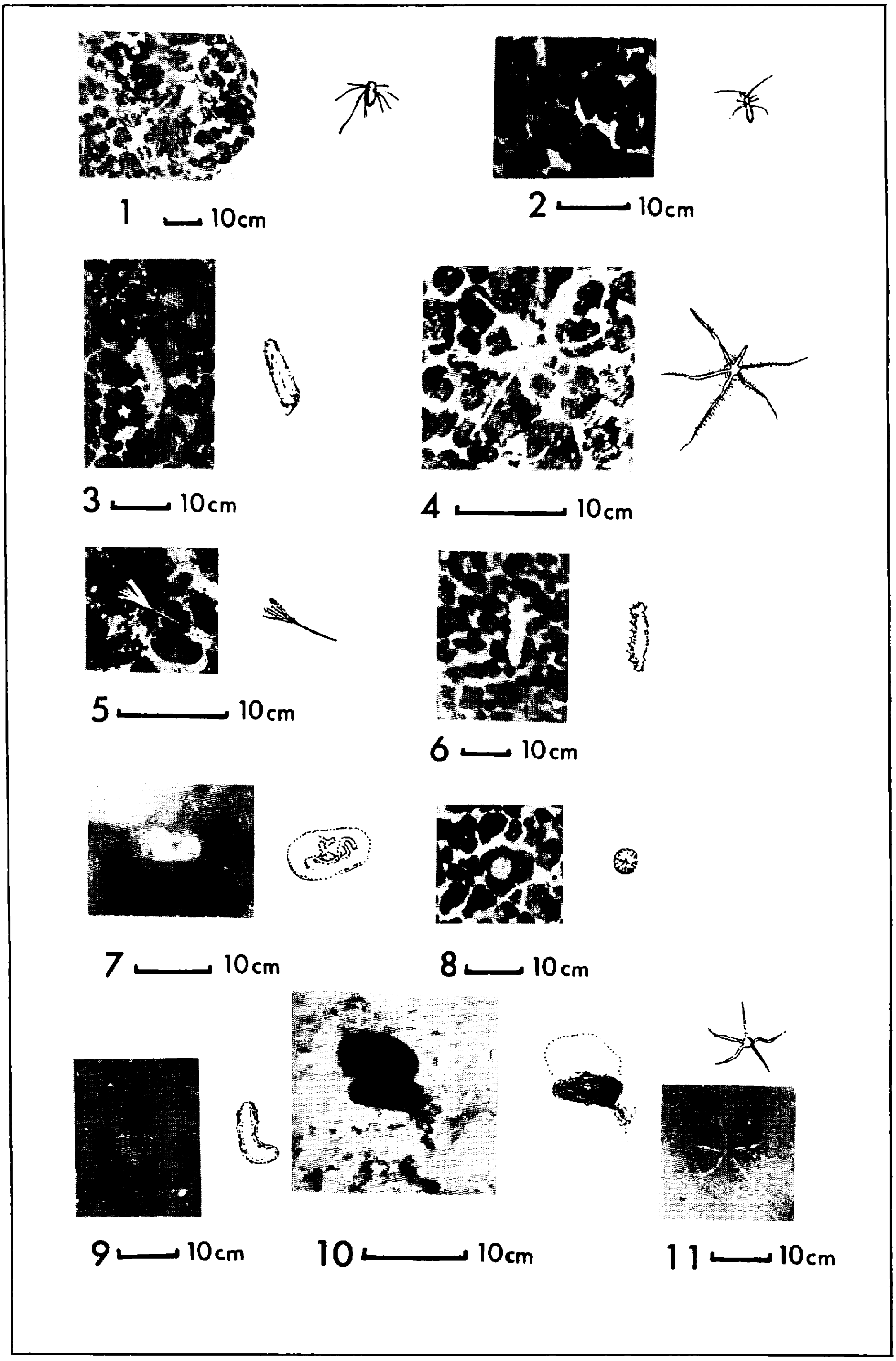

Fig. IX-9 Benthonic organisms photographed at Sts. 408A-1 (1–8) and 414A-3 (9–12). The explanations are given in the text.

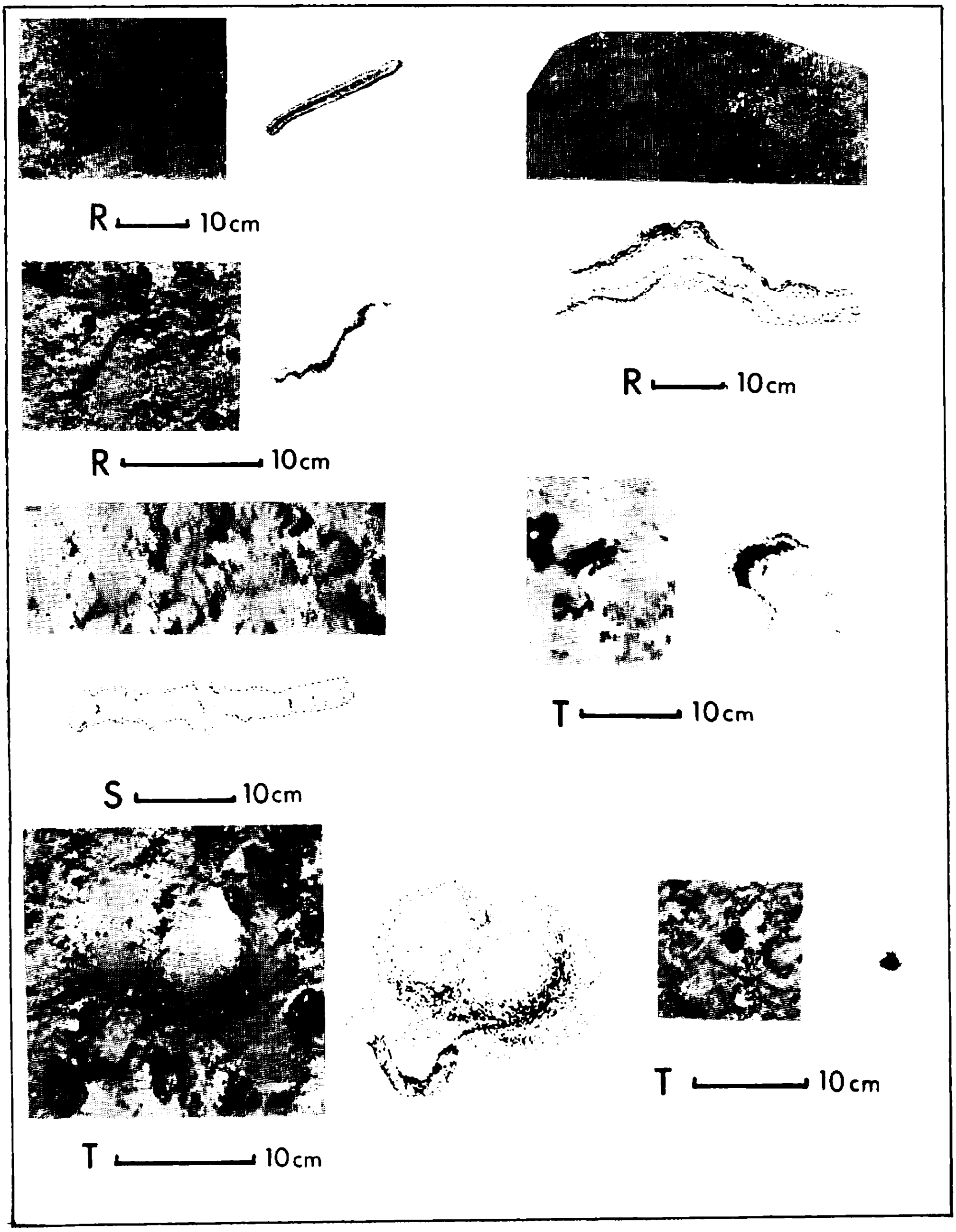

Fig. IX-10 Trails and burrows at St. 414A-3.
a, repichnia: b, cubichnia: c, domichnia

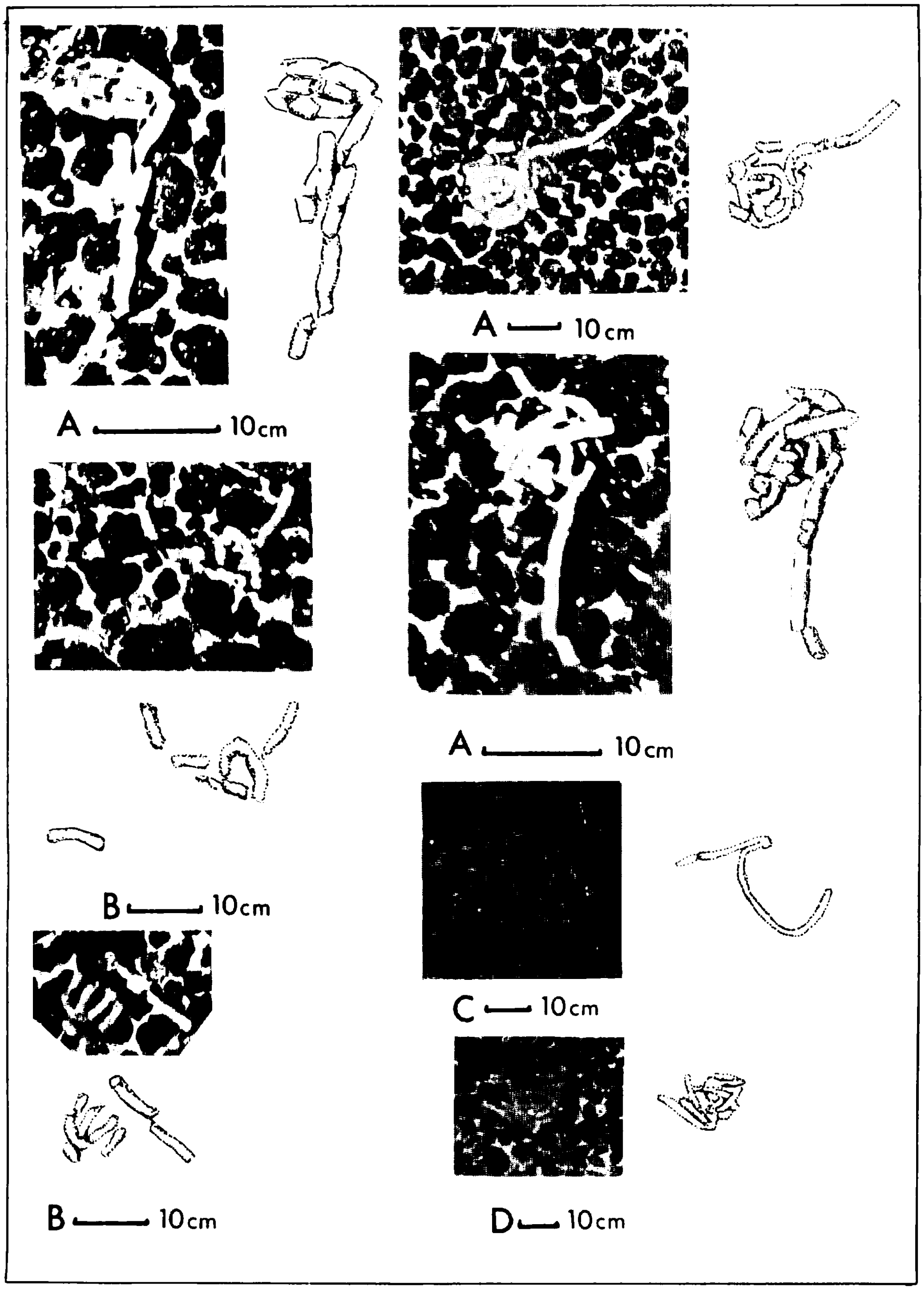

Fig. IX-11 Coprolites from St. 408A-1 (types A-D).

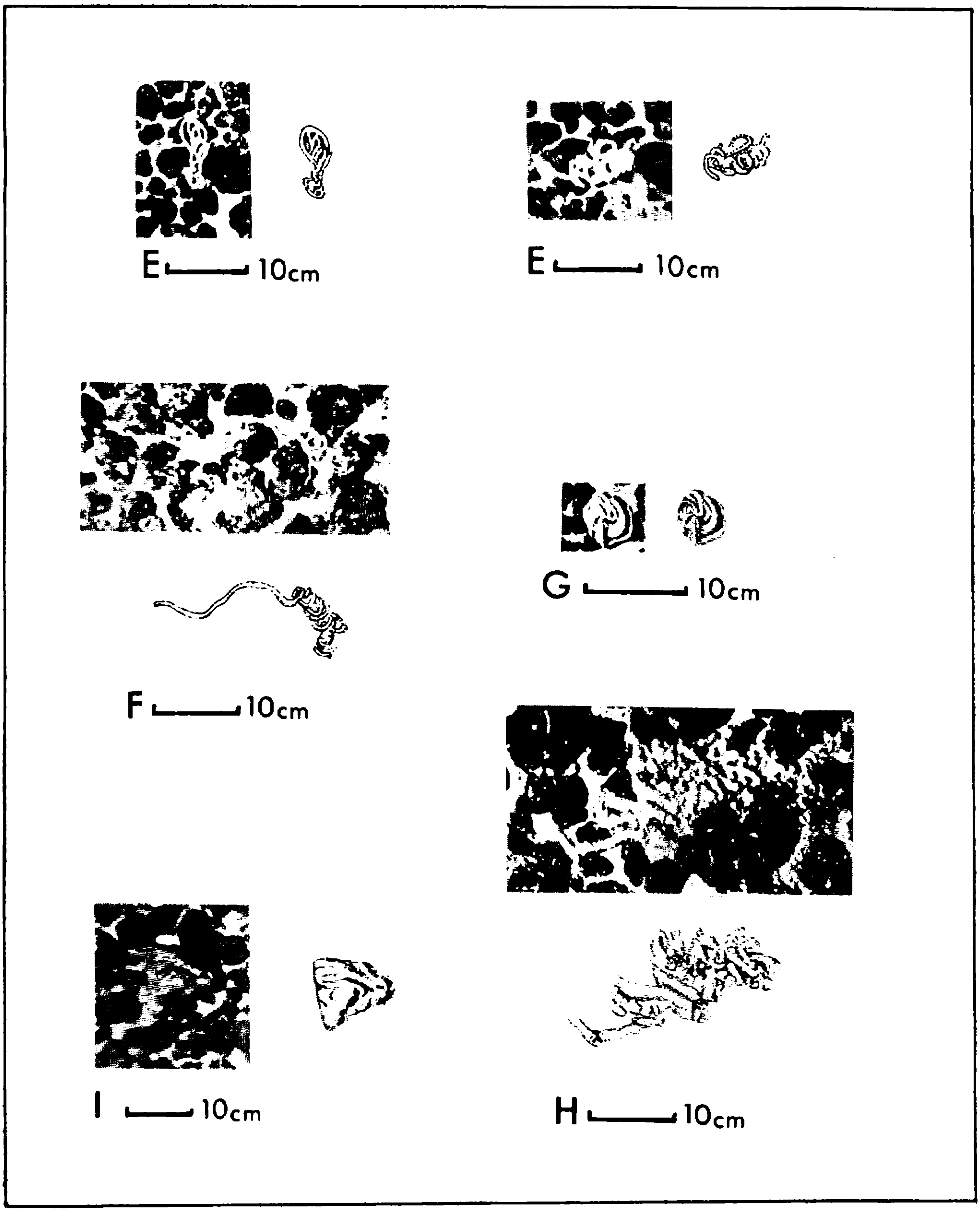

Fig. IX-12 Coprolites from St. 408A-1 (types E-H).

Types A and E are rather abundant, being found in fourteen and nineteen frames respectively in the total 147.

At St. 414A-3, the coprolites include eight tentative forms (J-Q in Figs. IX-13 and 14) which are either similar to or somewhat different from those at St. 408A-1. Here, types J, M, and, L are occasionally found, and particularly type M, which numbers 3–5 per unit surface area.

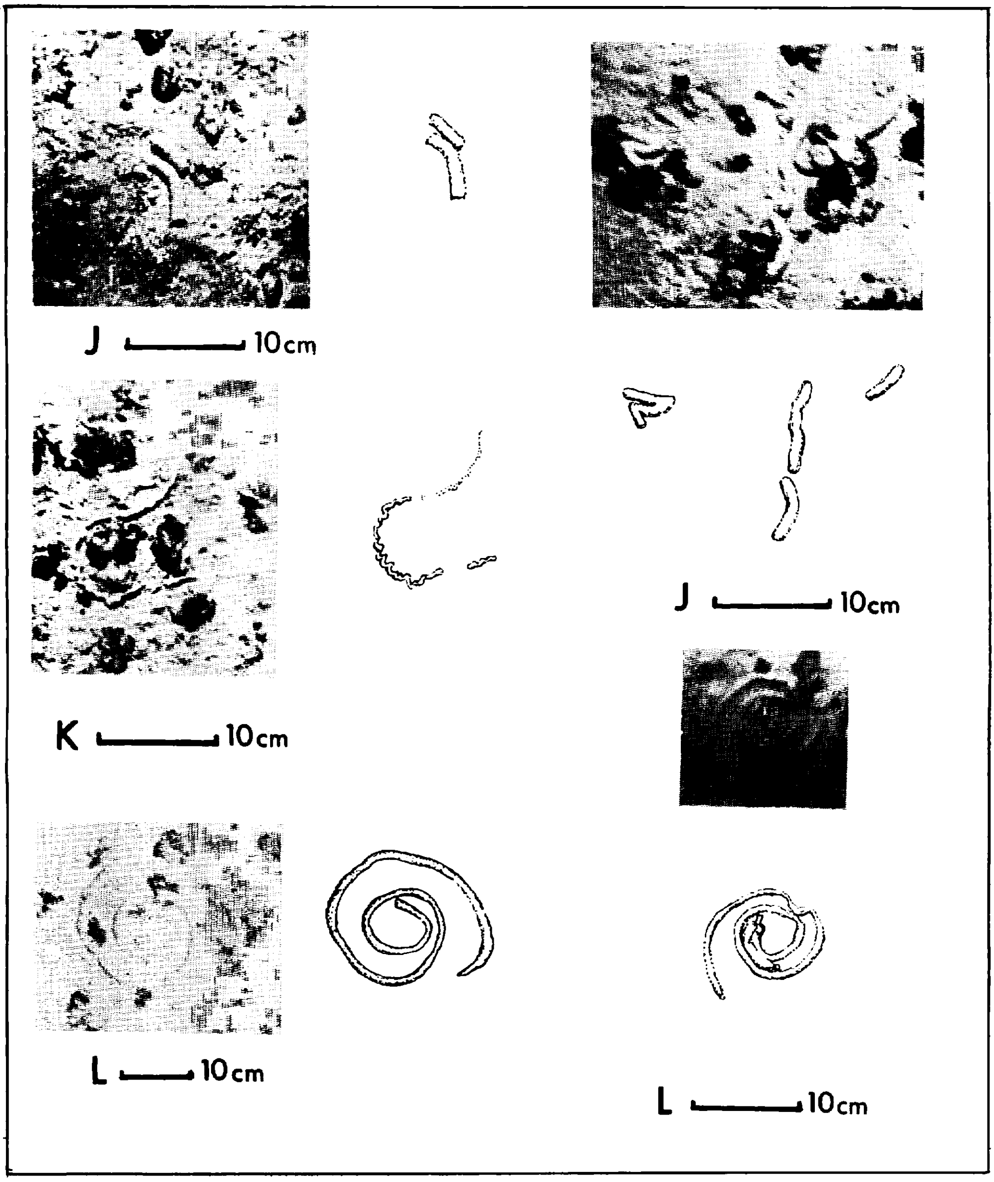

Fig. IX-13 Coprolites from St. 414A-3 (types J-L).

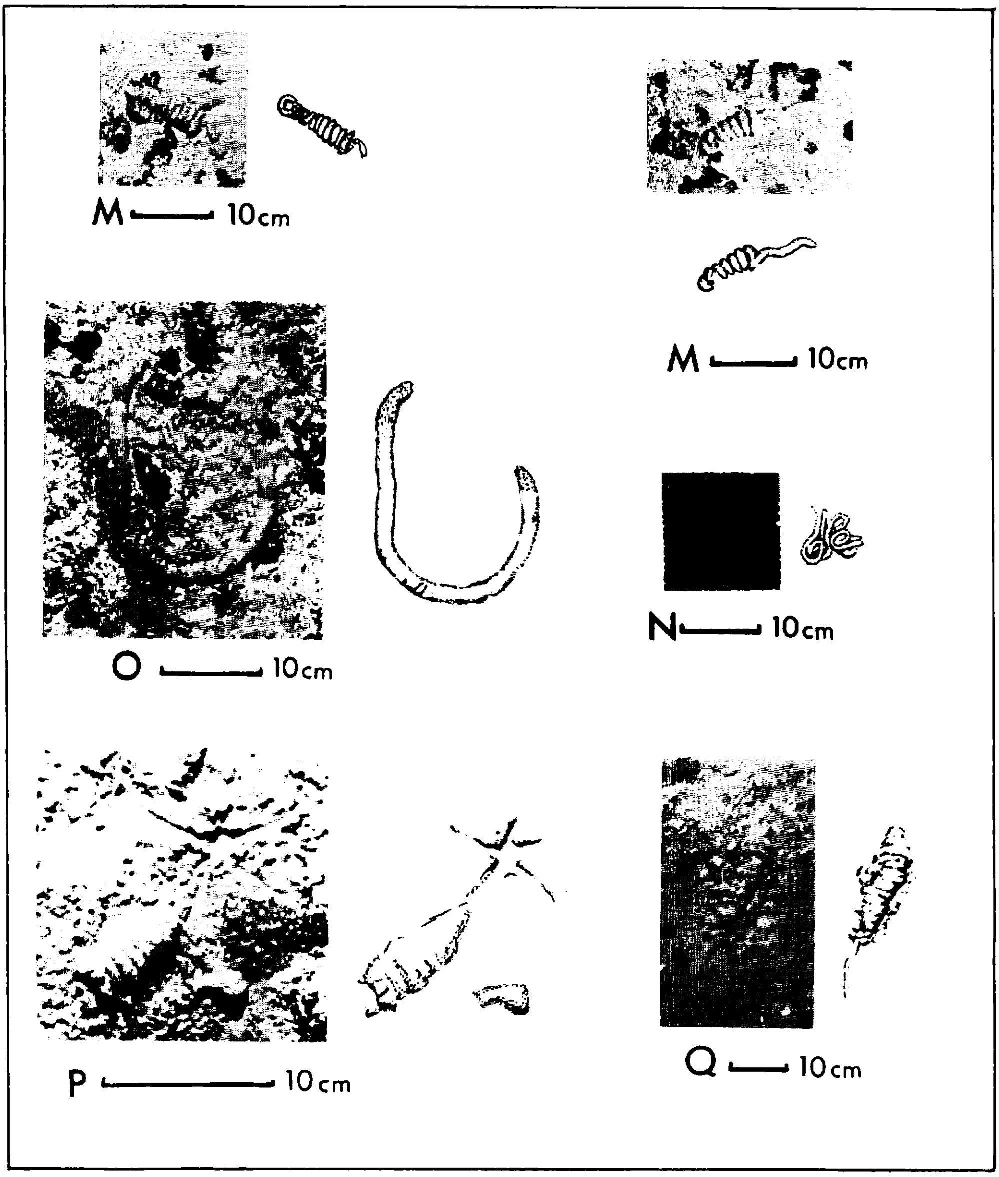

Fig. IX-14 Coprolites from St. 414A-3 (types M-Q).
Ophioroid-shaped impression is found together with P type coprolite in the lowest figure of left-hand.

All the types from both the stations are characterized by respective shape of lump. Some are rather regularly coiled, but some are complicatedly shaped with irregular coils, and the others show a rather simple shape elongated like a simple arc.

Among them, type A has a length of 50–60 cm and a width of 1.0–1.5 cm, forming a coiled lump-like shape at one end and a stretched projection at another. It would be reasonable to assume that coprolites of this type were produced by relatively large organisms. Type B looks like a part of type A, having a similar width. On the other hand type E is characterized, as well as types F and G, by a smaller length and width, the latter of which is only about 3–5 mm.

Among the types found in St. 414A-3, type J somewhat resembles type B from St. 408A-1. Type N, which is smaller, is similar to type E. Type M, the general form of which resembles types Q (? and P) in its coiled aspect with an elongated tail, is somewhat similar to type F, although the dimensions and details of shape are different.

EWING and DAVIS (1967) who classified *lebensspuren* into many morphological types described some forms of coprolite, and a few of the coprolite types seem to be similar to those from the Central Pacific stations. Type M here named has a very similar form to Group IIA5 of EWING and DAVIS, which were reported from the bottom at a depth of 1,900–5,949 m. Type L is somewhat similar to their Group IA1, the same form of which was reported by SEILACHER (1967) existing on the present sea bottom at a depth of 3,500 m. Also, types P and Q may be possibly correlated with Group IA6 found at a depth of between 223–5,951 m by EWING and DAVIS (1967).

The animals that produced the many types of coprolite are still unknown. However, if we assume that the difference of coprolite types at both the stations indicates different kinds of original animals, such differences might be related to size and/or composition of bottom sediment and feeding of animals, referring to the data on bottom materials by ARITA (see Chap. X of this report).

References

EWING, M. and DAVIS, R. (1967) Lebensspuren photographed on the ocean floor. *In* HEASEY, J. *ed., Deep Sea Photograph*, The Johns Hopkins Press, Baltimore, p. 259–294.

HANTZSCHEL, W. (1962) Trace fossils and problematica. *In* MOORE, R. C. *ed., Treatise on Invertebrate Paleontology. W. Miscellanea*, Geol. Soc. Amer. and Univ. Kansas Press, p. W177–W221.

HORN, D. R., HORN, B. M., and DELACH, M. N. (1973) Ocean manganese nodules. Metal values and mining sites. *Techn. Rept.*, no. 4, NSF GX 33616, IDOE, NSF, Washinton, D.C. 57p. (unpublished manuscript)

SEILACHER, A. (1953) Studien zur Palichnologie. I. Uber die Methoden der Palichnologie. *Neues Jb. Geol. u. Palaontol. Abh.*, Bd. 96, p. 421–452.

———— (1967) Bathymetry of trace fossils. *Marine Geology*, vol. 5, p. 413–428.

YAMAKADO, N., USAMI, T., HANDA, K., and KINOSHITA, Y. (1975) Deep sea photography. *In* MIZUNO, A. and CHUJO, J. (*eds.*), *Geol. Surv. Japan Cruise Rept.*, no. 4, p. 41–44.